Research Article

For reprint orders, please contact: reprints@futuremedicine.com

Nanomedicine

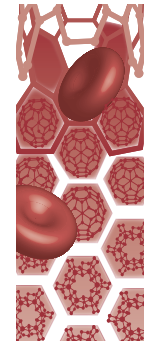

CEA-targeted nanoparticles allow specific *in vivo* fluorescent imaging of colorectal cancer models

Fluorescent imaging of colorectal tumor cells would improve tumor localization and allow intra-operative staging, facilitating stratification of surgical resections thereby improving patient outcomes. We aimed to develop and test fluorescent nanoparticles capable of allowing this *in vivo*. Dye-doped silica nanoparticles were synthesized. Anti-CEA (carcinoembryonic antigen) or control IgGs were conjugated to nanoparticles using various chemical strategies. Binding of CEA-targeted or control nanoparticles to colorectal cancer cells was quantified *in vitro*, and *in vivo* after systemic-delivery to murine xenografts. CEA-targeted, polyamidoamine dendrimer-conjugated, nanoparticles, but not control nanoparticles, allowed strong tumor-specific imaging. We are the first to demonstrate live, specific, *in vivo* imaging of colorectal cancer cells using antibody-targeted fluorescent nanoparticles. These nanoparticles have potential to allow intra-operative fluorescent visualization of tumor cells.

Keywords: colorectal cancer • dye-doped • IVIS imaging • live tumor imaging • silica nanoparticles • tumor markers

James P Tiernan[1,2], Nicola Ingram[1], Gemma Marston[1], Sarah L Perry[1], Jo V Rushworth[3], P Louise Coletta[1], Paul A Millner[‡,4], David G Jayne[‡,1,2] & Thomas A Hughes*[,‡,1]

[1]School of Medicine, University of Leeds, Leeds, LS9 7TF, UK
[2]John Goligher Colorectal Unit, St James's University Hospital, Leeds, LS9 7TF, UK
[3]School of Allied Health Sciences, De Montfort University, Leicester, LE1 9BH, UK
[4]School of Biomedical Sciences, University of Leeds, Leeds, LS2 9JT, UK
*Author for correspondence:
Tel.: +44 113 3431984
t.hughes@leeds.ac.uk
[‡]Authors contributed equally

Colorectal cancer resections are based on operations that have been performed for over 100 years, involving a radical mesenteric basin resection encompassing primary tumor, vasculature and lymphatics [1]. However, this 'one size fits all' approach may be inappropriate in an increasing proportion of cases. Currently only approximately 35% of patients undergoing colorectal cancer resections have nodal metastases [2], yet all of them undergo this radical resection. National bowel cancer screening programs have led to increases in diagnoses of small, early stage cancers, such as polyp and Dukes' A cancers [3]. These are less likely to have nodal metastases therefore resection with radical lymphadenectomy could be regarded as over-treatment. On the other hand, some have suggested that patients with nodal metastases may benefit from even more radical resections [4]. Unfortunately, at present there is no accurate method for assessing nodal status pre- or intra-operatively. A further issue is that accurate localization of small tumors during laparoscopic surgery, which is now in routine use in many centers [5], is especially problematic because of a lack of tactile feedback. These problems highlight the need for intra-operative tumor imaging that would aid tumor localization, and could also allow intra-operative staging of nodal metastases and thereby allow surgeons to stratify resection radicality to each individual patient.

Laparoscopic surgery provides an ideal platform for intra-operative fluorescent imaging. Camera systems can be modified simply to provide excitatory light of various wavelengths and fluorescent signals and white-light images can be detected and overlaid on-screen for real-time surgical guidance [6]. While technologies required for physical imaging are relatively well developed, the biological and nanotechnological requirements have lagged behind. We have previously investigated that colorectal cancer biomarker is suitable in this context and have determined that the tumor marker carcinoembryonic antigen (CEA) provides the best sensi-

Future Medicine part of fsg

tivity and specificity for colorectal cancer detection and localization [7]. We have now developed and validated a fluorescent nanoparticle that can target CEA to allow fluorescent tumor visualization. The requirements for such a particle are challenging. The particle must be bright enough to allow detection through tissue, while remaining sufficiently small to pass out of vasculature after intravenous delivery. Ideally, particles should have near-infrared emission wavelengths to increase tissue penetration and reduce auto fluorescence [8]. Particles must also have acceptable biotoxicity profiles, and resist photobleaching. We have focused on dye-doped silica nanoparticles, which have potential to meet these criteria. For the dye, we used NIR-664, which is an iodoacetamide dye with suitable excitation and emission characteristics (672 and 694 nm, respectively), as well as relatively good stability across different pH values and high quantum efficiency (23%) [9]. A number of studies have been published in which dye-doped silica particles have been investigated as agents to label cancer cells fluorescently [10–12]. However, a key concern is the nonspecific binding potentially exhibited by particles when using some conjugations to antibodies, meaning that use of appropriate nontumor targeted controls is critical. Here, we show the first successful and robustly controlled use of systemically delivered, targeted fluorescent nanoparticles for live *in vivo* colorectal cancer imaging. This represents a key stage in development of clinically practical intra-operative fluorescent imaging for colorectal cancer.

Materials & methods

Nanoparticle manufacture

Protocols were carried out at room temperature using Sigma-Aldrich (USA) reagents unless otherwise stated. Protocols were modified from previous publications [10–11,13]. 'Wash' steps: nanoparticles were pelleted by centrifugation (11,000 × g, 25 min), resuspended in wash solution using ultrasound sonication, repelleted and the supernatant discarded. 5 mg NIR664 (CA, USA) was dissolved in 6.25 ml 1-hexanol, and 3.25 µl (3-mercaptopropyl) triethoxysilane was added (stirred under nitrogen, 4 h). A total of 4.045 ml Triton X-100 was added to 15 ml cyclohexane, 1.6 ml 1-hexanol, 2 ml dye mixture and 960 µl water (stirred, 5 min). 200 µl tetraethyl orthosilicate was added (stirred, 30 min). One hundred and twenty microliters 28% [w/w] ammonia hydroxide was added (stirred, 24 h). 150 µl tetraethyl orthosilicate was added (stirred, 30 min). 20 µl ethanol was added and mixture was divided into two equal volumes before centrifugation (11,000 × g, 25 min). Particles were washed in ethanol (4×). 4 µl ethanol-suspended nanoparticles (2 mg/ml) were stirred with 4% (3-aminopropyl)triethoxysilane (3 h). Particles were washed in ethanol (2×), and once in 2-(N-morpholino)ethanesulfonic acid buffer (MES), pH 7, before resuspension in MES pH 7 at 2 mg/ml.

Antibodies

Humanized anti-CEA monocolonal antibody A5B7 was supplied by the Cancer Research UK Biotherapeutics Development Unit (Clare Hall Laboratories, UK). This antibody was raised against purified human CEA from human metastatic colon tumor tissue [14], and has been used previously in human clinical trials of CEA-targeted therapies [15,16] and in molecular pathology studies of human tissue [7]. Mouse monoclonal anti-digoxin IgG antibody (clone DI-22; Sigma-Aldrich, USA) was used as a negative, non-targeted, control.

Antibody conjugation

Succinimidyl-4-(N-maleimidomethyl)cyclohexane-1-carboxylate (SMCC): 500 µl of 4.8 mg/ml anti-CEA IgG antibody was added to 500 µl of 9.6 mg/ml 2-mercaptoethylamine (2-MEA). The mixture was incubated at 37°C for 90 min and then cooled rapidly on ice. 2-MEA was then removed using a 100 kDa spin centrifuge filter (Millipore, Billerica, USA); the mixture was centrifuged in 0.1 M PBS (14,000 × g for 2.5 min) and the eluent discarded. This was repeated seven times. The concentrated antibody solution was then retrieved by gentle centrifugation with the tube inverted (1000 × g for 30 s) and 0.1 M PBS was added to make the total volume up to 500 µl. The solution containing whole and reduced antibody fragments was reacted with nanoparticles immediately. 6 mg of fresh sulfo-SMCC was added to 4 ml of 1 mg/ml nanoparticles and stirred for 1 h. The maleimide-activated particles were then washed twice in PBS (10,000 × g for 15 min) to remove unbound sulfo-SMCC, and were resuspended at 2 mg/ml. The sample was split into two and 30 µg of reduced anti-CEA or antidigoxin was added to each tube. The reaction mixture was gently stirred for 2 h and then washed twice with PBS (6000 × g for 15 min). Finally, the particles were resuspended at 2 mg/ml and 0.1% (w/v) BSA added. The finished nanoparticles were stored in the dark at 4°C.

Poly[ethylene glycol] (PEG): A stock solution of 250 mM NHS-PEG-maleimide $(SM[PEG])_4$ was made by dissolving 100 mg in 680 µl DMSO. 8 µl of 250 mM $SM(PEG)_4$ solution was added to 5 ml of 2 mg/ml nanoparticles and reacted for 30 min with gentle mixing. Unreacted linker was removed by washing particles twice with PBS (pH 7.2, 10,000 × g, 15 min) and resuspending them in PBS at 2 mg/ml. The sample was divided into two. 30 µl of either anti-CEA or antidi-

goxin IgG was added for each mg of nanoparticles. The reaction mixture was incubated for 2 h with gentle mixing. The particles were then washed twice with PBS and resuspended at 2 mg/ml. A total of 0.1% (w/v) BSA was added and they were stored in the dark at 4°C.

1-Ethyl-3-[3-dimethylaminopropyl]carbodiimide hydrochloride (EDC): Nanoparticles were washed twice in DMF (10,000 × g, 15 min). They were then resuspended at 1 mg/ml in 15 ml 10% succinic anhydride dissolved in DMF. This was incubated under argon for 4 h with gentle stirring. The carboxylated particles were then washed three-times with distilled water. 10 mg of carboxylated nanoparticles were suspended in 5 ml of 0.1 M MES, 0.5 M NaCl, pH 6.0 and 1.92 mg EDC and 5.43 mg sulfo-NHS were added. They were incubated for 15 min with gentle mixing, after which the reaction was quenched by addition of 20 mM 2-MEA. Excess reactants were removed by washing the particles twice with PBS (6000 × g for 10min) and resuspended at 2 mg/ml in 0.1 M PBS. Ten micrograms of either anti-CEA or antidigoxin IgG was added for each mg of nanoparticles. The reaction mixture was incubated for 2 h with gentle mixing. The particles were then washed twice with PBS and resuspended at 2 mg/ml. 0.1% (w/v) BSA was added and particles were stored in the dark at 4°C.

PAMAM dendrimer: A total of 41.7 mg sulfo-NHS and 71.6 mg N-(3-dimethylaminopropyl)-N′-ethylcarbodiimide were added to 1 µmol polyamidoamine (PAMAM) dendrimer generation 4.5 (Dendritech, USA) dissolved in water, and the volume was made up to 1 ml with MES pH 6 (stirred, 25 min). Two milligram nanoparticles in MES pH 7 were added (stirred, 25 min). Particles were pelleted (16,000 × g, 8 min), six times and washed in MES pH 7 (twice). Samples were divided into two before addition of either 10 µg of A5B7 anti-CEA antibody (CRUK, UK) or antidigoxin IgG antibodies (Therapeutic Antibodies, UK). Particles and antibody were stirred (4 h) before addition of 100 µl of 0.1 M sodium hydroxide, pH 9.1. Particles were washed in 0.1 M PBS pH 7.2 (twice) before resuspension in 0.1 M PBS at 2 mg/ml. 2% (w/v) BSA was added and particles were stored (4°C, dark).

Scanning electron microscopy (SEM)

Images were captured using LEO1530 (Zeiss, Germany) or FEI Quanta (FEI, USA) field emission SEMs.

Tissue culture, confocal microscopy & image analysis

Cell lines were obtained from ATCC (USA). LS174T, LoVo and HCT116 cells were cultured in Advanced MEM (ATCC), F12K Nutrimix and RPMI1640 (both Invitrogen, USA), respectively, supplemented with 10% FCS and 1% L-glutamine at 37°C in 5% CO_2. Cells were seeded onto glass coverslips (Cellpath, UK) for 24 h. Cells were washed twice (PBS), fixed in 4% paraformaldehyde (30 min) and washed in PBS (3×). Coverslips were incubated in 0.1% (w/v) BSA (30 min) followed by PBS washes (3×). Coverslips were incubated with conjugated nanoparticles (1 mg/ml in PBS; 1 h, dark). Coverslips were washed in PBS (3×) and mounted using Depex (Waltham, USA). A Nikon A1R-A1 confocal microscope (Nikon, Japan) with NHS Elements software (v 4.0) was used. For each slide, cells were focused in phase mode in the center of one coverslip quadrant. Cy7 and phase filters were calibrated automatically for this first image only; settings (laser power and gain) were saved and used for all subsequent images. Phase/Cy7 z-stack images were captured for this first quadrant; distances between optical sections were chosen to allow similar numbers of sections for each line and the whole cellular depth to be included (0.5, 0.2 and 0.4 µm for LS174T, LoVo and HCT116, respectively). The microscope stage was then moved to another quadrant, focused and examined under white light only (thereby minimizing selection bias) and a further z-stack captured. This was repeated so five z-stacks were captured from each coverslip, from approximately each quadrant center and one from the center of the entire coverslip. Single optical sections to be analyzed were taken from half way between base and top of the cells: at 5, 1.4 and 4.8 µm from the base for LS174T, LoVo and HCT116, respectively. Fluorescence was quantified using tiff images with ImageJ v1.42q (NIH Freeware, USA). Membrane fluorescence (per µm) was determined by measuring the cell circumference, masking the cytoplasm and normalizing to background. This procedure was followed for five z-slices per cell line/particle type. Maximum image projection measurements were obtained by compressing all sections from each z-stack into a single image, and measuring mean fluorescences of the entire cell areas.

In vivo assays

All procedures were licensed by UK Home Office and were carried out in accordance with local ethical review. 4–6 weeks old BALB/c nu/nu female mice (Charles River, UK) were injected subcutaneously with 1.5×10^6 LS174T cells to the flank. When tumors reached approximately 10 mm diameter, mice were randomized to either CEA-targeted or control IgG conjugated-nanoparticles (50 mg/kg suspended in 100 µl PBS via tail vein under general anesthesia). Fluorescent images were captured using IVIS imaging (filters: excitation 672 nm, emission 694 nm; Perkin Elmer, USA) under anesthesia. Fluorescence measurements (radiant efficiency in $p/s/cm^2/sr/\mu W/cm^2$) were

taken using Living Image (v4.3.1, Caliper Life Sciences, USA); tumors were traced as regions of interest and mean quantum efficiency measurements taken, calibrated to background.

Statistics

Analyses were performed using in SPSS (SPSS, USA).

Results

Nanoparticle manufacture, antibody conjugation & physical characterisation

Protocols for manufacture of dye-doped silica nanoparticles encasing NIR664 dye were developed from published work [10–11,13]. Four separate protocols for conjugation of particles to antibodies were developed based on chemical linkers SMCC, PEG, EDC or PAMAM dendrimers, each of which has been reported to allow successful conjugation [13,17–19]. A schematic of the particles is shown in Figure 1A. Particles were characterized using scanning electron microscopy (Figure 1B). Unconjugated particles had a mean diameter of 57 nm and were relatively homogeneous (SD 7 nm), indicating that particles were consistently of a suitable size for intravenous delivery to tumors. Antibody-conjugated nanoparticles (data shown for PAMAM dendrimer-conjugated only) had an equally suitable mean diameter of 71 nm.

PAMAM dendrimer-conjugation allows antibody-targeting of nanoparticles *in vitro*

We assessed whether our four conjugation strategies allowed targeting of nanoparticles to cancer cells using tumor-specific antibodies. Nanoparticles were conjugated to antibodies specific for either CEA, since this marker is highly sensitive and specific for colorectal cancer detection [7], or the glycoside digoxin, as a negative control. Binding of antibody-conjugated nanoparticles to three different colorectal cancer cell lines *in vitro* (LS174T, LoVo and HCT116) was quantified using confocal microscopy (Figure 2 & Supplementary Figure 1, see online at www.futuremedicine.com/doi/suppl/10.2217/nnm.14.202). Fluorescence was first quantified on single optical sections through the middle of the cells. Nanoparticles conjugated using SMCC or PEG did not demonstrate any significant antibody-dependent tumor cell binding, although nonspecific binding was seen with both CEA- and control IgG-targeted particles (Supplementary Figure 1A & B). Similarly, nanoparticles conjugated using EDC showed very poor antibody-dependent tumor cell binding, with only 1.7-fold greater binding of CEA-targeted nanoparticles as compared with control in only one cell line (LoVo, $p = 0.017$; Supplementary Figure 1C). More encouragingly, conjugation via PAMAM dendrimers allowed strong tumor-specific targeting, with CEA-targeted nanoparticles demonstrating 12.3-, 8.0- and 3.2-fold greater fluorescence than control in LS174T, LoVo and HCT116 cells, respectively ($p < 0.002$; Figure 2A). Fluorescence was also quantified throughout the depth of the cells using maximum projection images, which compress the signals seen in individual optical section into one image. A similar pattern of successful CEA-targeted fluorescence was observed ($p < 0.0002$; Figure 2B).

CEA-targeted nanoparticles allow *in vivo* fluorescent imaging of colorectal xenografts

Next, we assessed whether these nanoparticles would allow *in vivo* tumor imaging. LS174T xenografts were established in nude mice and mice were injected intravenously with either CEA-targeted nanoparticles (n = 3) or control IgG nanoparticles (n = 3). Fluorescence was

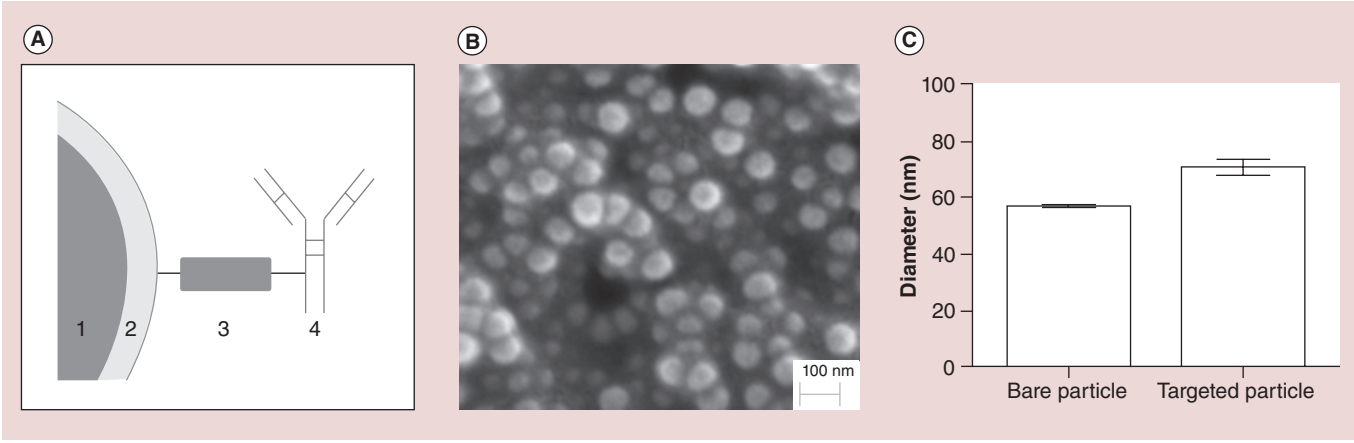

Figure 1. Nanoparticle characteristics. (A) Dye-doped silica nanoparticles conjugated to IgG antibodies via chemical linkers. 1: fluorescent core; 2: silica shell; 3: biochemical linker; 4: antibody. **(B)** Field emission scanning electron microscope image of unconjugated particles (magnification: 1×10^5). **(C)** Diameters of 50 randomly-selected unconjugated particles or anti-CEA-conjugated particles were quantified from electron microscope images (means with standard deviations; significance tested using unpaired t-tests).

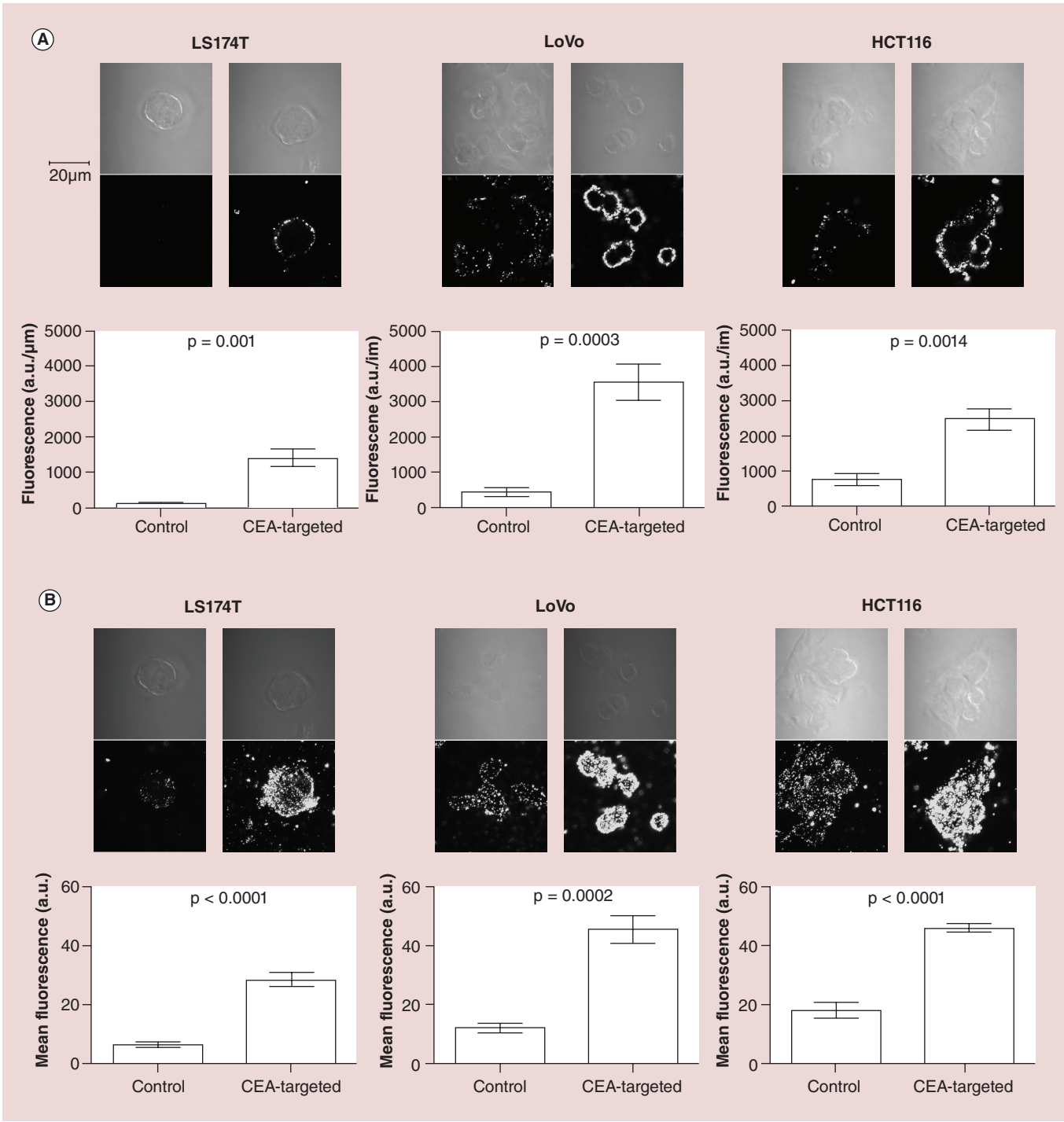

Figure 2. Dye-doped silica nanoparticles conjugated to anti-carcinoembryonic antigen antibodies via PAMAM dendrimers allow specific fluorescent imaging of colorectal cancer cell lines *in vitro*. Three different colorectal cancer cell lines were incubated with either nanoparticles conjugated to anti-CEA, or to control antibodies. Images were collected using confocal microscopy and fluorescence was quantified. Representative images are shown (magnification: 63×): **(A)** phase contrast and fluorescent central optical sections; **(B)** phase contrast and maximum image projection. Graphs representing mean fluorescence (with standard deviations) are shown; significance was tested using unpaired t-tests.
CEA: Carcinoembryonic antigen.

quantified within specific organs/tissues (tumor or liver) noninvasively at time points from 1 min through to 72 h after injection. Hepatic fluorescence was observed in all mice, suggestive of hepatobiliary excretion, a feature

observed previously [20]. Liver fluorescence was evident at 6 h (mean 8.01 × 10^7 p/s/cm^2/sr/μW/cm^2) and peaked at 24 h (8.98 × 10^7 p/s/cm^2/sr/μW/cm^2) before reducing (48 h: 7.42 × 10^7 p/sec/cm^2/sr/μW/cm^2 and 72 h: 4.80 × 10^7 p/sec/cm^2/sr/μW/cm^2). Hepatic localization was confirmed by *ex vivo* imaging of isolated organs. There was no significant difference in liver fluorescence between mice injected with control particles and those injected with CEA-targeted particles at any time point (p ranging from 0.3 to 0.9, Mann–Whitney Test). Fluorescence in other mouse tissues was not seen for either control or CEA-targeted particles, demonstrating that the particles have negligible nonspecific or antibody directed binding to host cells. Substantial tumor fluorescence was detected in all mice injected with CEA-targeted nanoparticles from 6h post-injection (Figure 3). Mean tumor fluorescence increased over the whole experiment from 6 h (mean 0.62 × 10^7 p/s/cm^2/sr/μW/cm^2) to 72 h (mean 4.74 × 10^7 p/s/cm^2/sr/μW/cm^2), although increases were only small after 48 h. Mice injected with control IgG-targeted nanoparticles showed no tumor fluorescence above background at any point (Figure 3). Fluorescence in the CEA-targeted tumors was significantly greater than controls at every time point after and including 6 h ($p < 0.0001$, Wilcoxon Signed Rank Test). The continued accumulation of tumor fluorescence with the CEA-targeted nanoparticles for up to 72 h suggests that at least a proportion of the conjugated particles are stable in the circulation for a minimum of 72 h.

Discussion

Dye-doped silica nanoparticles, as used here, were originally described in a study targeting human leukemia cells *in vitro* [11]. The fluorescent nanoparticles were conjugated using cyanogen bromide to leukemia cell-specific antibodies and the authors presented comparative images of cells incubated with targeted and control nanoparticles, although fluorescence was not quantified. However, critically, the controls consisted of 'bare' nanoparticles, with no targeting antibody or linkers attached, as opposed to the more appropriate controls of nontargeting antibodies. This lack of robust controls represents a key and recurring issue in the field, which is of particular importance since we show nonspecific binding of antibody-conjugated nanoparticles is prevalent using some conjugation strategies (Supplementary Figure 1) while antigen-specific targeting is more problematic.

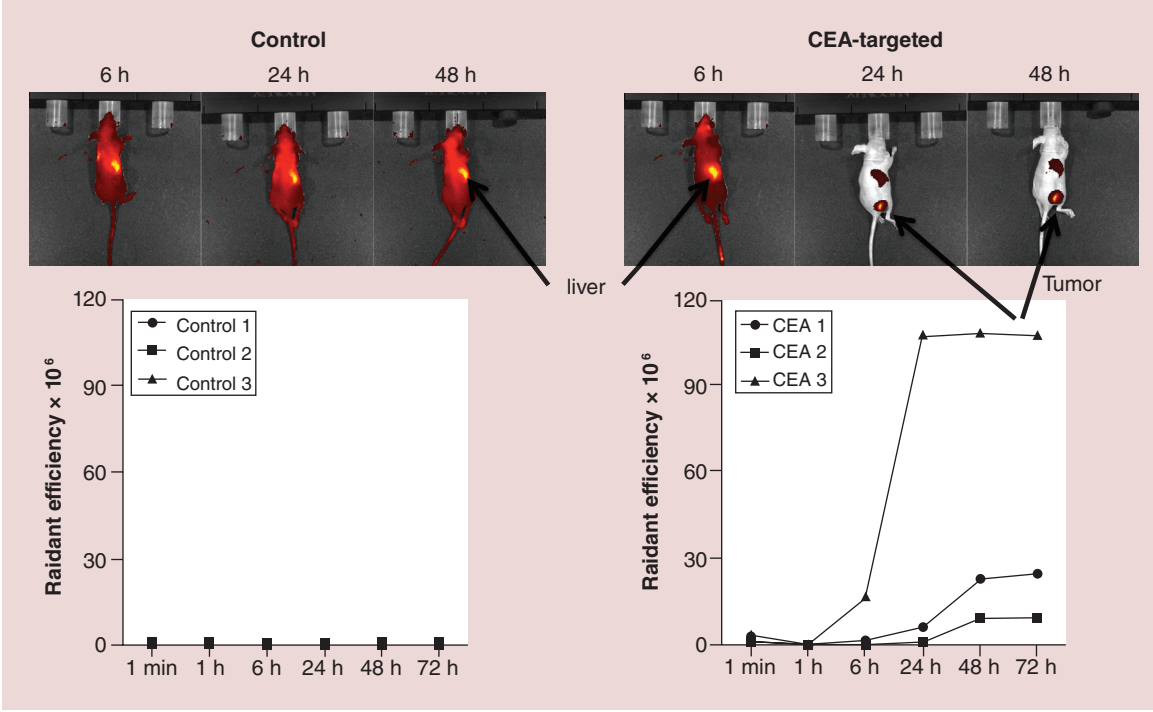

Figure 3. Carcinoembryonic antigen-targeted dye-doped silica nanoparticles allow live tumor-specific imaging *in vivo*. LS174T xenograft tumors were established in nu/nu balb-c mice. CEA-targeted or control IgG-conjugated particles were delivered systemically (50 mg/kg) and tumor fluorescence was measured using an *in vivo* imaging system small-animal imaging system at the time points shown. Representative images are shown of individual mice from each group (note these images were auto-exposed to enhance sensitivity, therefore depicted intensities are not comparable between images). Quantified data represent radiant efficiency for individual tumors in p/s/cm^2/sr/μW/cm^2.
CEA: Carcinoembryonic antigen.

Cyanogen bromide conjugation appears not to have been repeated in any other relevant work, however, several groups have published studies with a variety of antibody-conjugations, including streptavidin-biotin [21], glutaraldehyde [10] and EDC [19,22]. SMCC has also been used in similar contexts to conjugate reduced antibodies to nanoparticles using the free sulfhydryl group, with the aim of increasing specific targeting by improving antigen-recognition site orientation [17]. Conjugation using heterobifunctional PEG is a further option that can increase the particle circulating half-life by preventing reticulo-endothelial opsonization [18]. More recently dendrimers have also been used as linkers between nanoparticles and antibodies [13]. We have tested four of these linkers, focusing on EDC, since this has been used in the overwhelming majority of studies, SMCC and PEG, on the basis of the potential advantages described above, and dendrimers. In order to test the abilities of these conjugations to direct antigen-specific binding of nanoparticles we have performed carefully controlled and quantified analyses. We have previously demonstrated that CEA is the most appropriate biomarker for targeting colorectal cancer cells [7]. Therefore, here, we have used colorectal cancer cells as a target for nanoparticles conjugated to anti-CEA antibodies or to antidigoxin antibodies, with digoxin representing a negative-control antigen not present within these cells. We found only dendrimers to allow target-specific nanoparticle binding in all colorectal cell lines (Figure 2). Notably, SMCC allowed fairly strong binding without any suggestion of specificity, while EDC allowed weak specific binding in only one cell line (Supplementary Figure 1); these observations present concerns for the interpretation of previously published poorly controlled studies.

Having developed a fluorescent nanoparticle with genuine specificity for a surface antigen that is overexpressed in cancers, we then examined the potential for this to be used to image tumors *in vivo*, using colorectal cancer xenografts. We delivered particles systemically to simulate a pre-operative intravenous injection. CEA-targeted particles demonstrated, using *in vivo* imaging, significant time-dependent accumulation within tumors that was entirely absent for control-targeted particles ($p < 0.0001$) (Figure 3). Only two other studies have investigated specific targeting of dye-doped silica nanoparticles to tumors via systemic delivery: Tivnan *et al.* [12] used dendrimer-conjugated particles targeted to neuroblastoma, while Soster *et al.* [23] used PEG-conjugated particles targeted to colorectal cancer metastases, both in murine xenograft models. However, both studies used 'bare' nanoparticles as controls, which are potentially problematic in terms of demonstrating antigen-specific targeting, and both imaged fluorescence only on harvested organs *ex vivo*, which may relate to poor tissue penetration of fluorescence.

Conclusion

Our study is the first to use nanoparticles successfully to provide tumor-specific, live, *in vivo* fluorescent imaging in a murine model of colorectal cancer. Critically our work show great promise for clinical translation in the context of intra-operative imaging since fluorescence is bright, the antibody is humanized and has been used in clinical trials previously and silica nanoparticles appear to have favorable toxicity profiles. Furthermore, the technology is applicable to imaging any tissue or pathology using antibodies targeting appropriate specific biomarkers.

Future perspective

Fluorescent laparoscopic imaging of primary colorectal tumors and lymph node metastases is likely to become a routine procedure during colorectal resections within the medium term. However, demonstrating specific tumor labeling remains problematic in many published studied. Further work is required using rigorous controls in order to optimize specific tumor labeling before such technologies can be translated into the clinic.

Acknowledgements

The authors thank the Biotherapeutics Development Unit (Clare Hall Laboratories, Cancer Research, UK) for the A5B7 anti-CEA antibody.

Financial & competing interests disclosure

This work was supported by a CRUK fellowship to JPT, awarded through the Cancer Research UK Leeds Centre. The authors have no other relevant affiliations or financial involvement with any organization or entity with a financial interest in or financial conflict with the subject matter or materials discussed in the manuscript apart from those disclosed.

No writing assistance was utilized in the production of this manuscript.

Ethical conduct

The authors state that they have obtained appropriate institutional review board approval or have followed the principles outlined in the Declaration of Helsinki for all human or animal experimental investigations. In addition, for investigations involving human subjects, informed consent has been obtained from the participants involved.

Executive summary

Background

- Colorectal surgery could be aided by fluorescent labeling of tumor cells.

Materials & methods

- Dye-doped silica nanoparticles loaded with NIR664 dye were synthesized using a water-in-oil microemulsion technique.
- Anti-Carcinoembryonic antigen (CEA) IgGs or control IgGs were conjugated to nanoparticles using a variety of chemical strategies, including polyamidoamine dendrimers (PAMAM).
- Binding of CEA-targeted or control nanoparticles to colorectal cancer cells (LS174T, LoVo and HCT116) was quantified *in vitro* using confocal microscopy, or *in vivo* in the context of a murine xenograft model using noninvasive IVIS imaging.

Results

- CEA-targeted, PAMAM dendrimer-conjugated, nanoparticles allowed strong tumor-specific targeting *in vitro*, demonstrating up to 12-fold greater fluorescence than control IgG-targeted nanoparticles ($p < 0.002$).
- CEA-targeted nanoparticles demonstrated clear tumor-specific fluorescence in xenografts from 6 to 72 h after injection, as compared with only background fluorescence for control IgG-targeted nanoparticles ($p < 0.0001$).

Conclusion & future perspective

- These fluorescent nanoparticles show great promise for intra-operative imaging of colorectal cancers.
- The same technology could be harnessed for specific labeling of other pathologies using appropriate antibodies.

References

Papers of special note have been highlighted as:
• of interest

1 Jamieson JK, Dobson JF. The lymphatics of the colon. *Proc. R. Soc. Med.* 2(Surg. Sect.), 149–174 (1909).

2 Baxter NN, Virnig DJ, Rothenberger DA, Morris AM, Jessurun J, Virnig BA. Lymph node evaluation in colorectal cancer patients: A population-based study. *J. Natl Cancer Inst.* 97(3), 219–225 (2005).

3 Logan RFA, Patnick J, Nickerson C, Coleman L, Rutter MD, Von Wagner C. Outcomes of the Bowel Cancer Screening Programme (BCSP) in England after the first 1 million tests. *Gut* 61(10), 1439–1446 (2011).

4 Hohenberger W, Weber K, Matzel K, Papadopoulos T, Merkel S. Standardized surgery for colonic cancer: complete mesocolic excision and central ligation – technical notes and outcome. *Colorect. Dis.* 11(4), 354–364 (2009).

5 Association of Coloproctology of Great Britain and Ireland: National Bowel Cancer Audit Annual Report. (2013). www.acpgbi.org.uk/content/uploads/Bowel-Cancer

6 Cahill R, Anderson M, Wang L, Lindsey I, Cunningham C, Mortensen N. Near-infrared (NIR) laparoscopy for intraoperative lymphatic road-mapping and sentinel node identification during definitive surgical resection of early-stage colorectal neoplasia. *Surg. Endosc.* 26(1), 197–204 (2012).

7 Tiernan JP, Perry SL, Verghese ET *et al.* Carcinoembryonic antigen is the preferred biomarker for *in vivo* colorectal cancer targeting. *Br. J. Cancer* 108(3), 662–667 (2013).

• **A rigorous investigation of which tumor markers are most appropriate for targeting for nanoparticle based imaging**

8 Weissleder R. A clearer vision for *in vivo* imaging. *Nat. Biotechnol.* 19(4), 316–317 (2001).

9 Mank AJG, Yeung ES. Diode laser-induced fluorescence detection in capillary electrophoresis after precolumn derivatization of amino-acids and small peptides. *J. Chromatogr. A* 708(2), 309–321 (1995).

10 Huang S, Li R, Qu Y, Shen J, Liu J. Fluorescent biological label for recognizing human ovarian tumor cells based on fluorescent nanoparticles. *J. Fluoresc.* 19(6), 1095–1101 (2009).

11 Santra S, Zhang P, Wang KM, Tapec R, Tan WH. Conjugation of biomolecules with luminophore-doped silica nanoparticles for photostable biomarkers. *Anal. Chem.* 73(20), 4988–4993 (2001).

12 Tivnan A, Orr WS, Gubala V *et al.* Inhibition of neuroblastoma tumor growth by targeted delivery of MicroRNA-34a using anti-disialoganglioside GD(2) coated nanoparticles. *PLoS ONE* 7(5), e38129 (2012).

• **Xenograft model apparently showing specific tumour targeting of nanoparticles but using inappropriate controls.**

13 Gubala V, Le Guevel X, Nooney R, Williams DE, Maccraith B. A comparison of mono and multivalent linkers and their effect on the colloidal stability of nanoparticle and immunoassays performance. *Talanta* 81(4–5), 1833–1839 (2010).

• **Previous use of dendrimer linker between nanoparticle and antibody.**

14 Harwood PJ, Britton DW, Southall PJ, Boxer GM, Rawlins G, Rogers GT. Mapping epitope characteristics on carcinoembryonic antigen. *Br. J. Cancer* 54(1), 75–82 (1986).

15 Dawson PM, Blair SD, Begent RH, Kelly AM, Boxer GM, Theodorou NA. The value of radioimmunoguided surgery in first and second look laparotomy for colorectal cancer. *Dis. Colon Rectum* 34(3), 217–222 (1991).

16 Meyer T, Gaya AM, Dancey G *et al.* A phase I trial of radioimmunotherapy with 131I-A5B7 anti-CEA antibody in combination with combretastatin-A4-phosphate in advanced gastrointestinal carcinomas. *Clin. Cancer Res.* 15(13), 4484–4492 (2009).

17 Lee J, Choi Y, Kim K *et al.* Characterization and cancer cell specific binding properties of anti-EGFR antibody conjugated quantum dots. *Bioconjug. Chem.* 21(5), 940–946 (2010).

18 Owens DE 3rd, Peppas NA. Opsonization, biodistribution, and pharmacokinetics of polymeric nanoparticles. *Int. J. Pharm.* 307(1), 93–102 (2006).

19 Zhao XJ, Hilliard LR, Mechery SJ *et al.* A rapid bioassay for single bacterial cell quantitation using bioconjugated nanoparticles. *Proc. Natl Acad. Sci. USA* 101(42), 15027–15032 (2004).

20 Souris JS, Lee C-H, Cheng S-H *et al.* Surface charge-mediated rapid hepatobiliary excretion of mesoporous silica nanoparticles. *Biomaterials* 31(21), 5564–5574 (2010).

• **Xenograft model apparently showing specific tumour targeting of nanoparticles but using inappropriate controls.**

21 Lian W, Litherland SA, Badrane H *et al.* Ultrasensitive detection of biomolecules with fluorescent dye-doped nanoparticles. *Anal. Biochem.* 334(1), 135–144 (2004).

22 Wu H, Huo Q, Varnum S *et al.* Dye-doped silica nanoparticle labels/protein microarray for detection of protein biomarkers. *Analyst* 133(11), 1550–1555 (2008).

23 Soster M, Juris R, Bonacchi S *et al.* Targeted dual-color silica nanoparticles provide univocal identification of micrometastases in preclinical models of colorectal cancer. *Int. J. Nanomed.* 7, 4797–4807 (2012).